

Article

Clinical diagnosis of pancreatic cancer using biomarker methylation and nanotechnology-supported deep learning techniques

Ravindran Nair Padma Sumithra^{1,*}, Thankamony Saradhadevi Sivarani²

- ¹Department of Computer Science and Engineering, Amrita College of Engineering and Technology, Erachakulam, Nagercoil, Tamil Nadu 629901, India
- ² Department of Electrical and Electronics Engineering, Arunachala College of Engineering for Women, Manavilai, Nagercoil, Tamil Nadu 629203, India
- * Corresponding author: Ravindran Nair Padma Sumithra, r.p. sumithra@gmail.com

CITATION

Sumithra RNP, Sivarani TS. Clinical diagnosis of pancreatic cancer using biomarker methylation and nanotechnology-supported deep learning techniques. Journal of Biological Regulators and Homeostatic Agents. 2025; 39(4): 3854. https://doi.org/10.54517/jbrha3854

ARTICLE INFO

Received: 24 June 2025 Revised: 10 July 2025 Accepted: 26 August 2025 Available online: 2 December 2025

COPYRIGHT



Copyright © 2025 by author(s). Journal of Biological Regulators and Homeostatic Agents is published by Asia Pacific Academy of Science Pte. Ltd. This work is licensed under the Creative Commons Attribution (CC BY) license. https:// creativecommons.org/licenses/by/4.0/

Abstract: Background: The extensive study of clinical health systems is creating a paradigm for the newest computer-based systems that are emerging. Pancreatic cancer, which cannot be allowed to be treated efficiently once diagnosed and is frequently unanticipated due to its position in the belly below the stomach, is one of the most prevalent tumors that is believed to be irreversible. Biological therapies, sometimes referred to as immunotherapies or targeted therapies, are used to treat pancreatic cancer in order to control hormone pathways, target certain cancer cells, or strengthen the immune system. Method: Pancreatic cancer is the fourth leading cause of cancer deaths, and there currently is no reliable modality for the early detection of this disease. Here, identifies cancer-specific promoter DNA methylation of BNC1 and ADAMTS1 as a promising biomarker detection strategy meriting investigation in pancreatic cancer. Nanoparticles directly target tumor cells, allowing their detection and removal. It also can be engineered to carry specific payloads, such as drugs or contrast agents, and enhance the efficacy and precision of cancer treatment. This study develops a unique cascaded fully convolutional neural network (CFCNN) with Hybrid Krill Herd African Buffalo Optimization (HKH-ABO) mechanism for early pancreatic computed tomography (CT) image classification of pancreatic cancer. A new Wienmed filter is created for pre-processing the noisy CT image content after the system is successfully trained on pancreatic CT pictures. In addition, the proposed CFCN with the HKH-ABO pathway distinguishes between pancreatic cancerous and non-pancreatic cancerous forms of the disease. Results: The accuracy of the CFCNN for the analysis of pancreatic cancer was 98.87%, showing that the various volumes of the 3DIR-CAD datasets analyzed had a combined accuracy rate of 99% for training and 99% for testing. Conclusion: The combination of advanced biomarker identification, BNC1 and ADAMTS1 methylation, and nanoparticle-based targeting further enhances the precision and efficacy of pancreatic cancer diagnosis and treatment. As a result, advancements in medical study are steadily going in the direction of the installation of automation machines that determine the phases of cancers and, if directly touched, provide better guidance and therapy.

Keywords: cascaded fully convolutional neural network (CFCN); deep learning; hybrid krill herd African buffalo optimization (HKH-ABO); pancreatic cancer; Wienmed filter and 3DIR-CAD datasets

1. Introduction

An examination of patient medical records reveals the fact that one of the most challenging diseases, cancer, occasionally asserts that it is incurable. Because it can be brought on by alterations in the genes which control how sentient bodily cells function, it might be seen as a genetic disease. These epigenetic changes may be inherited, brought on by a healthy and balanced diet, or brought on by environmental factors including cigarettes, UV radiation, and other chemical pollutants that harm DNA. Pancreatic cancer is one of the malignancies with the worst prognosis, and unlike other cancers, no progress has been made in recent years. Surgery is the sole curative therapy, however, only 15%–20% of patients are suitable, and the risk of relapse is considerable. In advanced pancreatic cancer, there are limited first-line therapeutic choices and no validated biomarkers to aid in treatment selection. Biomarkers that could aid in the development of tailored therapies for pancreatic cancer. Thus, the purpose of this study is to provide an up-to-date viewpoint on biomarkers with therapeutic promise in pancreatic cancer [1].

The inhibitors, protooncogenes, and DNA repair genes are three distinct protein types that function as cancer catalysts that will be impacted by the genetic manipulation. A medical investigation identified certain malignancies as incurable, including breast cancer, lung disease, and hepatocellular carcinoma [2]. Distant metastasis illness is the term used to describe the cancer's propagation from its origin or frame of reference to other internal functions. Carcinoma is the result of cancer cells dispersing.

Convolutional neural networks (CNNs)-based methods for deep learning have shown a lot of promise for analyzing medical images [3]. In order to collect and analyze the information from the photos and develop a model that reflects the complex relationship connecting images and diagnoses, neural pathways are built on a stack of neurons made up of optimization techniques and parameters. In the imaging identification of a number of disorders, including skin cancer [4], macular degeneration, and liver cancers, the use of CNN has proven to be highly useful. Regrettably, there has not been a lot of research on CNN's potential value in pancreatic cancer early detection and diagnosis. Even the most skilled radiologist may have problems producing an early diagnosis of cancer tissues because the majority of them have ill-defined boundaries and irregular shapes on CT. The nano-based cancer images are an effective diagnostic approach and classified to detect cancer cells. It measures the size, color, and shape of the cancer cell. Various types of tumors such as benign (non-cancerous) and malignant (cancerous), or tumors from different tissues and organs can be recognized and distinguished from one another, along with the position of the tumor, and to calculate tumor growth. These can be identified using the labeling tool to detect biomarkers of cancer cells in the human body. An early stage can help to reduce cancer cells spreading to other parts of the body by applying the nanomaterial block [5].

In this work, we demonstrate how to classify images using a cascaded fully convolutional neural network (CFNN) and extract characteristics from images in several medical domains. The Convolutional Neural Network model with Hybrid Krill Herd African Buffalo Optimization (HKH-ABO) has been created and tested using operational computed tomography (CT) data. Each image was divided into a separate convolutional layer. In order to identify images of pancreatic cancer, a comparable study investigates how a variable affects a Convolutional Neural Network's construction procedures. It is difficult to categorize "thicker" images with CFCNN. Although CT images are frequently used in diagnostic imaging, unintended abnormalities can still be created. The boundary prevents these items from appearing in the pictures. The

pancreatic cancer cells in the medical image's unwanted peaks are removed using the thresholding method.

The main contributions of the paper are the following:

- The computer was originally used to work using a collection of CT pancreatic images.
- Identify cancer-specific promoter DNA methylation of BNC1 and ADAMTS1 as a promising biomarker detection strategy meriting investigation in pancreatic cancer
- To suggest a HKH-ABO with CFCNN to classify pancreatic cancer using deep learning techniques employing CT images.
- Pre-processing Wienmed filter methods were initially applied to enhance the
 pancreatic pictures' quality. The CT scans' training distortion was eliminated in
 the pre-processing layer, and error-refined input images were acquired.
- Using the HKH-ABO algorithm and the CFCNN architecture to create high-level characteristics that can be immediately extracted from data.
- In the end, experimental findings have been used to improve accuracy levels in terms of precision, recall, specificity, sensitivity, and error rate.

The majority of the essay is detailed as follows: the sections listed below will be formatted as follows: Section 2 goes into the literature review for our proposed approach and other pertinent information. Section 3 explains the methodology technique; Sections 4 and 5 describe the investigation's results and discussions; and Section 6 summarizes the conclusion of the study and suggestions for future research.

2. Related works

The difficulty of cancer screening and risk classification has recently given rise to considerable interest to deep learning approaches. The majority of PC-related studies, nevertheless, have focused on the analysis of well-structured file formats, such as genomics and graphics data, up to this point. A graph-based technique to learning algorithms, for instance, was employed in Al-Fatlawi et al. [6] to infer the architecture of transcription factors systems that have been uniquely related to progressively advanced disease of PC. The investigators of refs. [7–9] were able to distinguish acute cholecystitis from Pancreatic Cancer (PC) by combining deep-learning-based sequencing approaches with biomarker and RNA-based variations obtained from endothelial cell samples. Both computerized pancreatic feature segmentation from CT scans and techniques for PC segmentation utilizing endosonographic images are outlined in the literature [10]. For structured time-series parameters like Electroencephalogram (EEG) measurements, the usefulness of data mining techniques for information retrieval tasks has also been shown [11].

Numerous blood biomarker enzymes, including lactate dehydrogenase, γ -glutamyl transferase, and alkaline phosphatase, have been utilized to identify conditions like myocardial infarction, liver dysfunction, and prostate cancer. Activity-based screening of blood samples revealed changed single-molecule activity patterns of CD13 and DPP4 in individuals with early-stage pancreatic cancers. The work demonstrates the effectiveness of single-molecule enzyme activity screening in identifying biomarkers based on protein functional changes [12]. The loss of potentially predic-

tive data is irreparable as a result of these input data limitations, which typically call for substantial human pre-processing. Moreover, the classic "black-box" prediction algorithms are problematic due to their lack of interpretability, which lessens their utility for medical applications to tackle the inter complexity of EHR data, a number of AI-based modeling algorithms based on language modeling have recently been developed [13]. For illustration, employing semi-structured data set of smear photos and a combination of long short-term memory and convolutional networks, the authors of [14] construct higher models for ovarian cancer detection using semi-structured time series of smeared photos. These trickier strategies have not, as far as we know, been applied to the PC risk prediction challenge. Due to the richness of knowledge included in unstructured multimodal biological data, the general problem of data fusion in this field has recently become a focus of active research; an overview of current developments can be obtained in Azad et al. [15].

The challenge of creating mathematical models to describe and explain to unseen database containing substantial design differentiations nearly equivalent to the model training examples, which might also occur, for instance, because of variations in legislative compliance across different institutions, is among the most important challenges in this field. López-Zambrano et al. [16] propose a taxonomy over several levels of repeatability and examine the factors that affect errors at each level in a bid to fix these issues. The authors of Gutiérrez et al. [17] demonstrate how this strategy improves the generalization ability of the framework when it comes to prognostications about how students will communicate with educational software by developing an epistemological structure for going to weigh how so much numerical simulations rely on high-level characteristics with more semantic information. A crucial topic that has been examined in Farag et al. [18] in the setting of knowledge fusion is the authenticity of information saved under multisensory fusion in the absence of unreliable or erroneous sources.

Several platforms have used a variant of the U-Net architecture to segment the pancreas. Fully convolutional network (FCN) and U-Net have been employed by other frameworks to build more complex models. Using a training FCN-based fixed-point model, for instance, determines the general pancreatic region and iteratively refines it. Using boundary maps created by trustworthy intraglomerular using random forests, pancreas areas are first segregated using holistically multi-layered networks. Furthermore, Jain et al. [19] segments the CT pancreas using dense convolution layer, which reduces computational burden by using fewer non-zero parameters. Deep neural networks, in combination with recurrent networks of neurons and long short-term memory (LSTM) systems, were utilized as well. A model that really can incorporate uncertainty in the recurrent segmentation process was recently suggested using the shadowing sets theory. Slices along axial, sagittal, and coronal axes are occasionally utilized to incorporate spatial 3D additional context through 2D categorization by integrating the output of all 2D networks, for instance, using plurality casting [20].

Recently, further publications have been published on pancreas segmentation [21–22]. The difficulty of segmenting the pancreas for medicinal or diagnostic purposes is reflected in the interest in the topic. In this area, researchers have chosen to use the hierarchical atlas methodology since the anatomy of the pancreas has undergone considerable permanent deformation. Wolz et al. [23] used an architectural path that passes through the skull along the splenic and superior peritoneal veins

to pinpoint the exact location and composition of the pancreas. They employed 200 alternative methods, including classification and regression trees, the AdaBoost racist and discriminatory learning algorithm, the course classifier, and a fine classification algorithm based on the probabilistic spatial model of the pancreas and surrounding tissues and vasculature. They were able to get a global temperature distance of 1–2 mm utilizing a dataset of 40 CT scans and the classifier segmentation approach. Taha and Hanbury [24] segmented 12 organs, including the pancreatic, using categorization, identification, and level creation. The analysis of 10 non-contrast CT scans revealed an average overlap of 32.5%. A highly autonomous pancreatic segmentation algorithm was published by Okada et al. [25] using three-phase contrast enhancement CT datasets, which was a significant advancement over their prior work. When compared to standard CT, three-phase contrast-enhanced images offer more segmented information. To precisely localize the pancreas, they used a high-profile deformable landmarks model with a low-profile probabilistic patients' health probability atlas.

Combining morphology and image intensity approaches, the final classification was created. Twenty three-phase CT cases were evaluated using the Jaccard index; the results demonstrated a mean of 57.9%. Chu et al. [26] used a hybrid method that combines local volumetric weighted structural segments with atlas loading on a hierarchy, regional, and regional level to segment various organs. The study made use of 150 CT scans from 114 males and 36 women. They used the cross-validation technique of omitting one. The suggested method yielded a 69.6 16.7 Dice coefficient [27] for pancreatic localization in 150 individuals. By merging the spatial links of body organs with probabilistic atlases, Placido et al. [28] carried out multi-organ identification. For surface topography, hierarchical information and the shape models of nearby organs such as the heart, brain, lungs, pancreas, appendix, and the inferior vena cava are used. The pancreatic delineation over 28 cases of especially in comparison to CT datasets produced a Dice index of 46.6%. An approach for segmenting multiple organs using probability maps of the world with spatially variable parameters is presented in Brachi et al. [29]. For the pancreas in particular, they apply a position-based weighing algorithm and space division to address the great variability in organ form and location in various patients. Their findings on 100 transabdominal examples exist Dice indexes for the hepatic, heart, pancreatic, and kidneys of 95.1%, 91.4%, 69.1%, and 90.1%, respectively.

Nanomedicine has great potential in pancreatic adenocarcinoma, because of the ability of nano-formulated drugs to overcome biological barriers and to enhance drug accumulation at the target site. Moreover, monitoring of disease progression can be achieved by combining drug delivery with imaging probes, resulting in early detection of metastatic patterns. Brachi et al. [29] describe the latest development of theragnostic formulations designed to concomitantly treat and image pancreatic cancer, with a specific focus on their interaction with physical and biological barriers.

3. Methodology

The cornerstone for the automated method of healthcare pictures is the registering and recognition of features in an image using previously established measurements and retraining by a predetermined number of labeled images. To highlight the

architectural irregularities and deformations in the area of interest and to precisely identify the relationships between each tissue and body organ, an anatomical standards model is needed Release of Information (ROI). Here, a hierarchy atlas model is used to recommend a pancreas CFCNN assignment. At both the global and organ levels, the mathematical properties of position, scale, and rotations are evaluated for the mapping organs. The global atlas settings are transferred to the ensemble space to minimize the probability distance among coordinates. The characteristics from each map constituent are compared to the actual polygons received from the planned patient CT at the relevant role.

3.1. Biological treatment in pancreatic cancer

The **Figure 1** presents advances in understanding pancreatic tumor biology and the underlying mechanism of disease aggressiveness are providing clues, which may help to potentially improve diagnosis, treatment, and patient outcome. Some of the critical biological determinants in the development and progression of pancreatic cancer. Central to this pathway is the study of tumor biology, which influences early detection, treatment development, and ultimately leads to better clinical results.

3.1.1. Tumor biology as the central focus

Molecular mechanisms of solid cancer are very complex with different mechanisms taking place and affecting the tissue at different stages of the disease. The classic model of pancreatic cancer development describes morphological as well as molecular transformation from precursor lesions into invasive carcinoma. The standard nomenclature and diagnostic criteria for classification of duct lesions has primarily been based on grades of pancreatic intraepithelial neoplasia (PanIN).

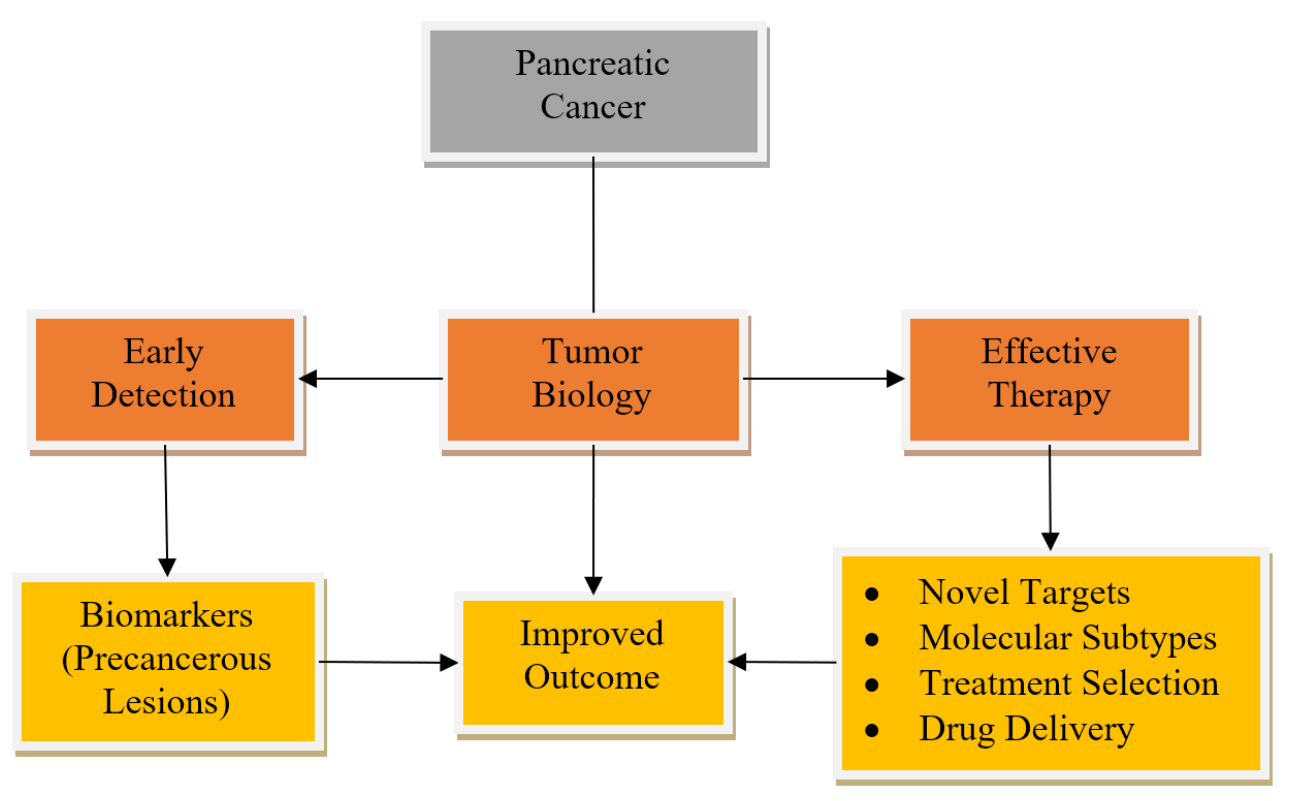


Figure 1. Block diagram for pancreatic tumor biology.

The grades 1A, 1B, 2, and 3 represent growing cytological atypia characterized by loss of polarity, nuclear crowding, enlarged nuclei, pseudo-stratification, and hyperchromatism. Each PanIN stage is characterized by a distinct pattern of molecular processes that are characterized by genetic irregularities that affect specific genes and genetic pathways. These study findings suggest that stratification of patients on the basis of the molecular signatures of their tumors could provide a means for predicting drug sensitivity.

3.1.2. Early detection through biomarkers

Ideally, biomarker analysis occurs prospectively as part of large randomized clinical effectiveness trials. Wherever possible, new studies including patients with pancreatic cancer should include biomarker testing as part of the translational component. The next best alternative is to do an accurately powered retrospective study of clinical trial material, but ad hoc research employing samples with insufficient clinical data should be avoided. To present, research has concentrated on drug transporters, drug-metabolizing enzymes, and proteins that inhibit or enhance the expression of drug-metabolizing enzymes as potential predictors of a patient's response to various treatments. As illustrated in **Figure 2**, the majority of studies and clinical trials have aimed to develop an affordable, non-invasive, or minimally invasive biomarker with high sensitivity and specificity for PDAC in order to enhance early detection and subsequent treatment. Biomarkers for PDAC can be classified as diagnostic, prognostic, and predictive. Will present a contemporary perspective on diagnostic indicators for early pancreatic cancer diagnosis.

3.1.3. Effective therapy via personalized approaches

On the right side, the diagram highlights how understanding tumor biology leads to effective therapy. This is achieved through several components:

Novel targets: Identifying specific genes or proteins involved in cancer growth provides targets for new drugs.

Molecular subtypes: Classifying tumors based on molecular characteristics allows for more accurate diagnoses and tailored therapies.

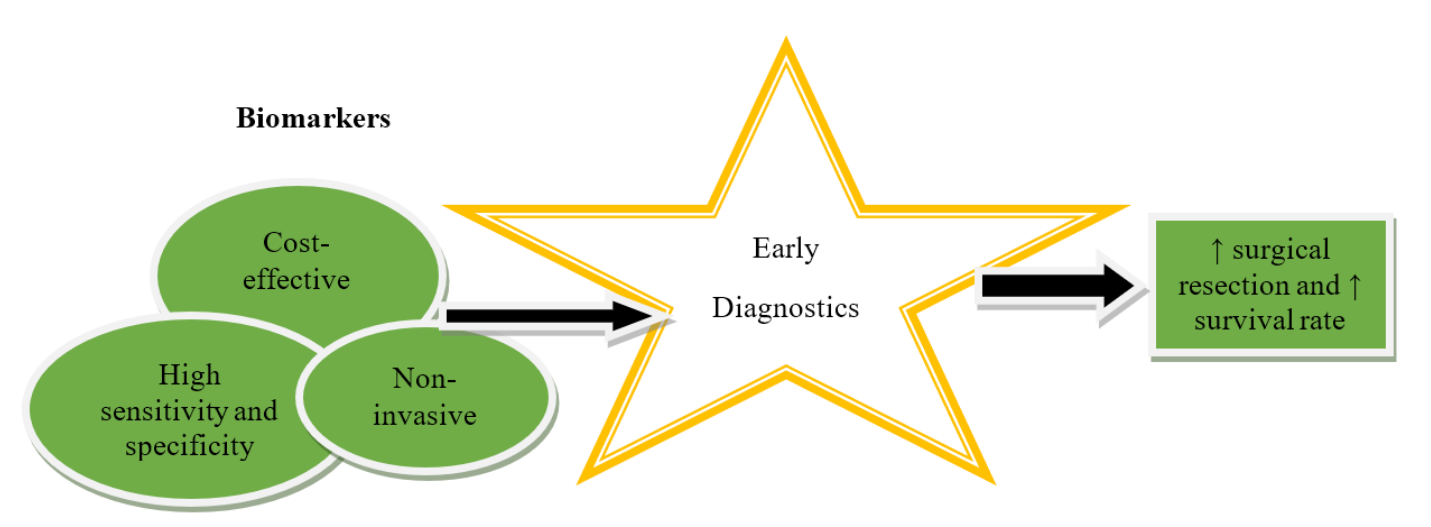


Figure 2. Characteristics required for biomarkers of pancreatic cancer.

Treatment selection: Tumor biology helps determine which treatments are likely to be most effective for individual patients.

Drug delivery: Liposomes, nanoparticles, and carbon nanotubes are the most popular drug delivery vehicles in the treatment of pancreatic cancer. These carriers can shield medications from degradation and successfully deliver them to their intended organs. Tumor markers are chemicals produced by cancer cells or normal cells in response to malignancy in the body. Healthy adults can have trace quantities of CA 19-9 in their blood. High levels of CA 19-9 are frequently indicative of pancreatic cancer.

Both early detection and effective therapy converge on the ultimate goal, i.e., improved outcome. This includes higher survival rates, reduced side effects, and better quality of life. The diagram thus effectively illustrates how a deep understanding of pancreatic tumor biology is essential to overcoming the challenges posed by this lethal disease and improving the overall clinical management of patients.

3.2. Proposed nano-based CFCNN with HKH-ABO mechanism

Pancreatic cancer generally affects the pancreatic cells of women and results in tumor formation, which worsens women's health. The 2018 research states that pancreatic cancer affects 50% of Indian women and kills 58% of people worldwide. Thus, this study created the CFCNN with the HKH-ABO strategy for earlier pancreatic cancer prediction. To train and test the system, pancreatic CT scans are initially used. These pictures are also before using a special Wienmed filter to remove any undesirable noise components. The constructed CFCNN with the HKH-ABO model is used to process the pancreatic CT dataset in order to summarize the cancerous cells and their types at an earlier stage. In addition, the designed CFCNN with the HKH-ABO mechanism improves the accuracy of classification. As a result, the new technique detects and categorises pancreatic cancers at an early stage. **Figure 3** illustrates the developed strategy's process steps.

3.3. Nanotechnology

Nanotechnology has enormous benefits in a variety of medical sectors, with diverse applications in diagnosis and treatment. Nanotechnologies are now widely regarded as having the potential to improve a variety of industries, including medication research, water purification, information and communication technologies, and the manufacturing of stronger and lighter materials. Nanotechnologies are the processes of creating and manipulating materials at the nanometer scale, either by scaling up from single atom groups or refining or reducing bulk materials. Nanoparticle-based technologies focus on enhancing the efficiency, sustainability, and speed of existing processes. This is achievable because, in comparison to standard industrial processes, nanoparticle-based technologies employ less material, much of which is already in a more "reactive" condition. The use of nanoparticles to deliver PSs has been demonstrated to improve PDT efficiency while decreasing off-target negative effects.

It may change the size, shape, surface properties, targeting, and composition of smart nanoparticles in response to both endogenous and external stimuli produced by the cell, as illustrated in **Figure 4**.

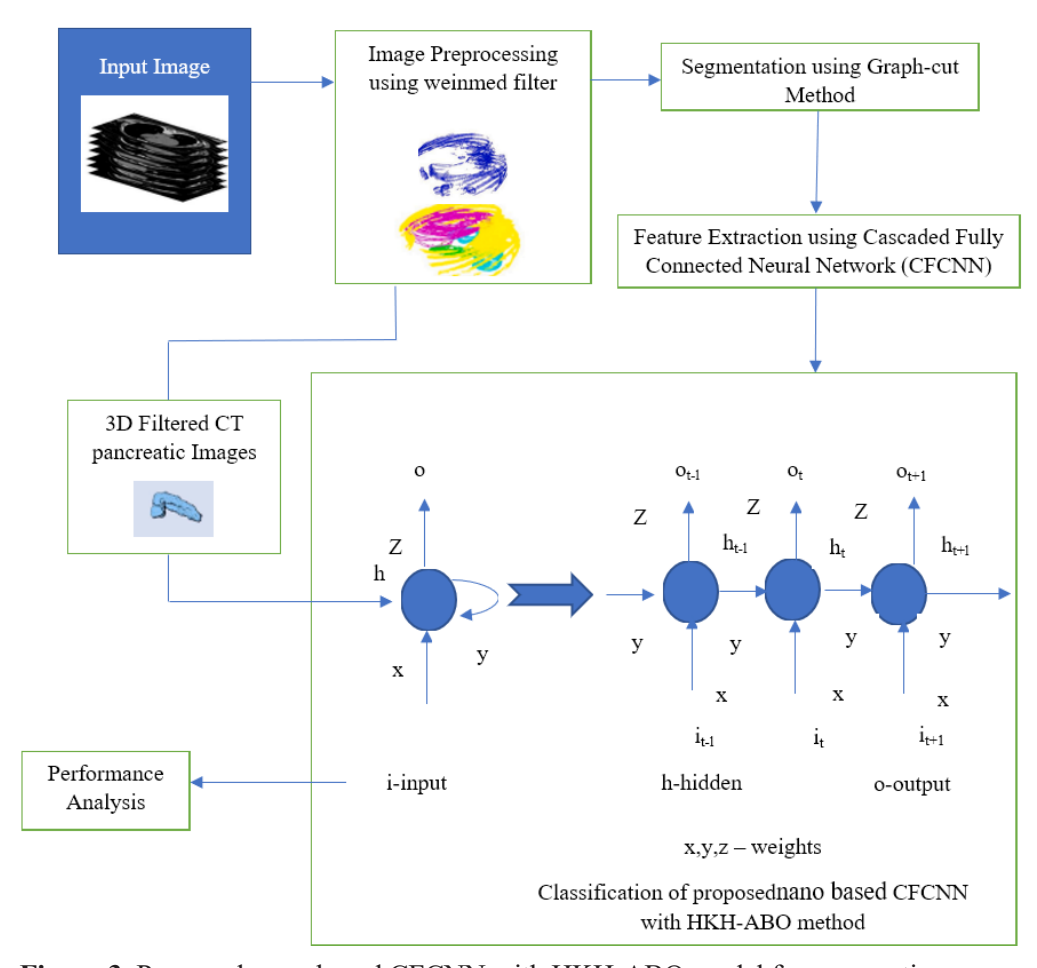


Figure 3. Proposed nano-based CFCNN with HKH-ABO model for pancreatic cancer.

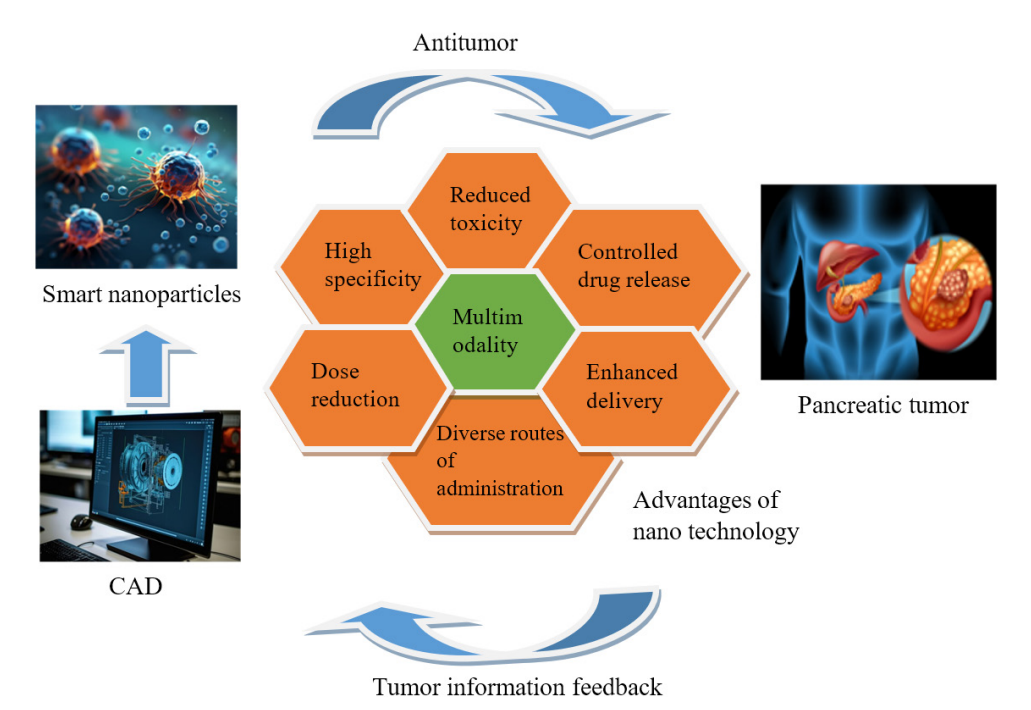


Figure 4. A schematic illustration of smart nanoparticles for pancreatic tumor treatment.

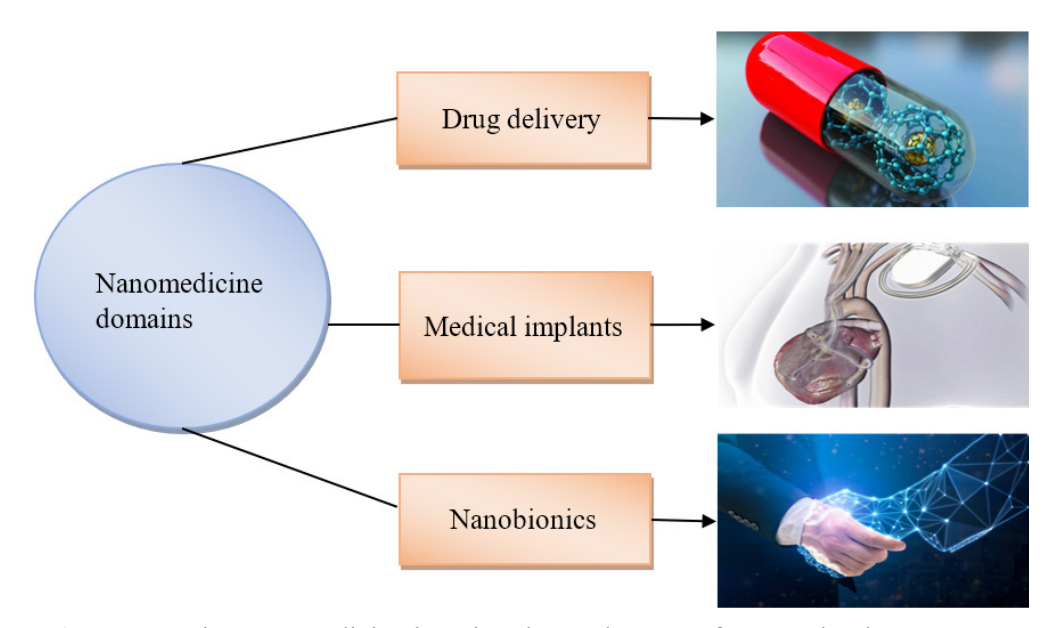


Figure 5. Major nanomedicine imaging that makes use of nanotechnology.

3.3.1. Medical applications of nano imaging

Nanotechnology-based medical imaging is being used to track transplanted stem cells. Medical imaging of stem cells necessitates the use of contrast chemicals. However, current contrast agents have issues such as metabolic deterioration within the body and photo bleaching when photochemical destruction occurs. Along with classic fluorescence imaging and CT, nanoparticles have been employed to create another type of nanoscale medical imaging. **Figure 5** shows three important nanomedicine fields that benefit from nanotechnology.

Nanotechnology offers a broad range of applications. However, its medicinal uses are likely the most important, as they directly benefit human lives. Nanotechnology has some genuinely game-changing applications in medical treatment. Examples of how nanoparticles and nanomaterials are used in medicine include the following:

- Nanoparticle applications include the development of nanorobots capable of repairing or healing at the cellular level.
- Nano sponges are polymer nanoparticles covered with a red blood cell membrane that remove toxins from the bloodstream.
- Nanoflare, a customized nanoparticle, locates genetic targets in cancer cells.
 They are programmed to generate light when a specific genetic target is detected.
- Nanoparticles, along with radiotherapy, are utilized to control tumors locally.

3.4. Image preprocessing

All sagittal CT scans of an individual's pancreas or pancreatic cancer were manually labeled by one of two experienced abdomen radiologists so that the model could be trained, validated, and tested using open-source software. Because of the pancreatic border multiple structures and tissues and also pancreatic cancers sometimes have unclear borders with the interstitial, so the intercoder differences between the meaningful degree of the pancreas and the tumor may exist. Hence, the radiologist verified that the pancreas and tumor in the images that were tagged were in accordance before continuing with the

image processing and analysis. Two hundred and fifty Hounsfield units were the window's width and level (HU). The spots that were not pancreatic or tumors were deleted from further inspection after the images were standardized to the range [0,1] using linear interpolation. Using the linear estimation method, the images were then cropped into rectangular subdomains with origins in the greatest axis (x-y) plane. Between both the limits on the right and left, the windows traveled along the x-axis, then descended a distance down the y-axis until beginning to move along the x-axis once more in the direction of the opposing border, finally coming to rest in the bottom-right corner. The movement length was set to twice of the patched dimension to produce overlapped patches, which increased the variance and amount of the training data. Patches with only normal pancreatic tissue were classified as non-cancerous, while areas with pancreatic cancer were labeled as cancerous.

3.5. Graph-cut segmentation

The initial pancreatic segmentation identifies areas on the organ's outermost layer that have an undetermined structure according to surface elements that were paired to the training evaluation in the first stage. Each doubtful site is given a unique mark using principal components analysis, and because S has a cut-off of 0.2, any intra-patient variability can be taken into the investigation. A quick labeling level was employed to "boost" the models have been developed on the curve of the CT images after the initial procedure largely segmented the livers. The seeds were consequently positioned in the middle of the labeling. Segmentation is improved by using a geometrical outline with flexible geometry. The process continues up to the increase or decrease by S 0.2 or up until the increase or decrease between those repetitions. The procedure recommends using a graph-cut method to segment the pancreas in characterizing modest hepatic tumors. The segmentation of larger and smaller structures, such as blood arteries and varied cancer patterns, presents a challenge since the decreasing bias issue affects graph cuts in their most fundamental form. The schematic cuts have improved the segmentation of large intestines, and tumors and capillary differ significantly from person to person. On the other hand, cancers are typically curved and parabolic. Equations (2) and (3) must be used to calculate the tumor vessels and blobs (3).

$$E_{\text{vessels}} = -\ln\ln(^{2}\text{v}(p,)),$$
with $v = \left\{ \left| \lambda_{2} \right| + \lambda_{1}, \text{ if } \lambda_{1} < 0 \left| \lambda_{2} \right| - \frac{\lambda_{1}}{4} \right\}$
if $\lambda_{2} < 0 < \lambda_{1} < 4 \left| \lambda_{2} \right|$

$$(1)$$

$$E_{blobs} = -\ln \sigma_{max}$$
 (w),

with $\lambda_3 > 0$;

$$w = e^{-(\lambda/\lambda^{3-l})}.$$

3.6. Classification of proposed nano-based CFCNN method

The U-Net architecture is used to implement the soft mark likelihood maps P. By fusing temporal and geographic information into a 19-layer co-evolutionary communications infrastructure with the trained U-Net curve in the 3DIRCAD data set and merging the results into one network architecture, the U-Net design enables precise pixel estimate. **Figure 6** shows the volume change in pancreatic cancer over time as well as the cancer loading, which is significant for a number of individuals.

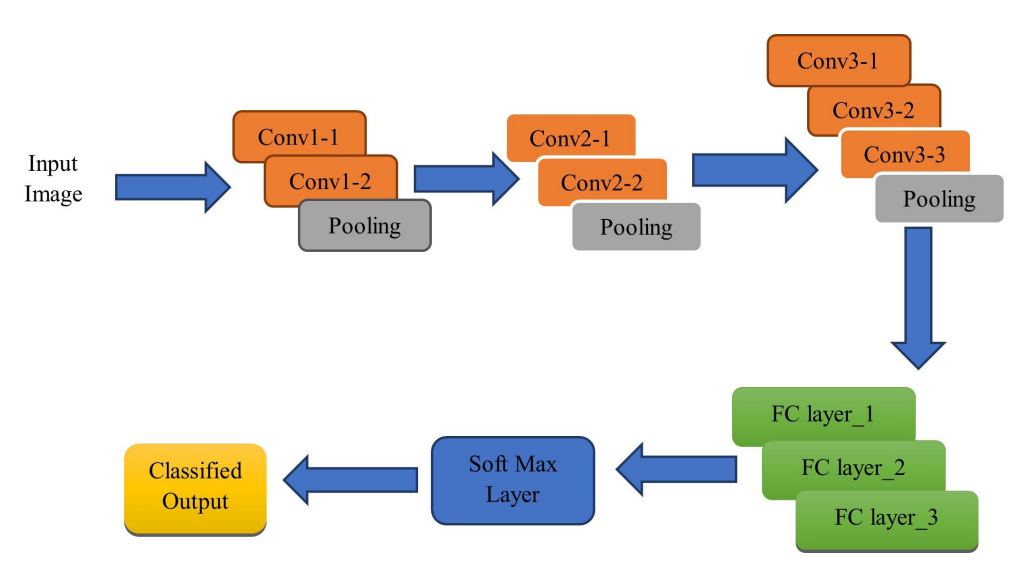


Figure 6. A designed and evaluated cascaded convolutional neural network.

Also, according to Research Dice, the overall effectiveness of automatic segmentation has increased to 53%. The simultaneous separation of the digestive system and the lesion is a skill that the U-Net has perfected. One of our most important contributions is the cascade training of CFCNN, which allows CFCNN to learn distinguishing properties only once during training in order to finish a multiclass classification, improving classification efficiency overall. U-Nets and other types of CFCNNs recognized the supplied data's hierarchical system, which led to the development of the approach. The layer stacks of the CNN architecture are changed toward to the selected categorization in an information manner rather than manually assembling living thing facial appearances for the distinguishing of various tissue kinds. Instead of learning from a broad CT abdominal scan filtration, U-Net learns from a filtering that is particular to the identification and segmentation of the pancreas by cascading two U-Nets.

Moreover, the pancreatic ROI helps to remove lesions from the body. The pancreatic network in the abdominal region is as follows:

- This network's research only focuses on finding and analyzing distinguishing characteristics in pancreatic segmentation.
- Then, a next network is trained to segment the lesions in the acquired pancreas picture.
- After being separated in Step 1, the pancreas is compressed and s new in Step 2 to produce an input dimension suitable for the cascade U-Net. The second U-Net is likely to concentrate on discovering the unique traits of the lesion rather than fragmenting the pancreas history.

Pseudocode for Cascaded Fully Convolutional Neural Network

Initiate the partitioning procedure. Start with the segmented image's characteristics. Let x be a pixel feature. $y_k = g_m(y_{m-1}) \text{ be the neuron layers}$ While x feature $>y_k$ $y_k = \text{ReLU } (x_m \otimes y_{m-1} + C_m)$ then $f(\theta) = m^y(\theta, y)$ End

After being separated in Step 1, the pancreas is compressed and s new in Step 2 to produce an input dimensionality suitable for the cascade U-Net. The second U-Net is likely to concentrate on discovering the unique traits of the lesion rather than fragmenting the pancreas ethicology.

3.6.1. Proposed pancreatic cancer classification using nano-based CFCNN with HKH-ABO

The 3DIRCAD CT dataset is processed using the CFNN with HKH-ABO framework, which could also classify the illness categories to identify the extent of the pancreatic cancer. Here, the initial classification accuracy of the CFNN's classification layer is enhanced by the HKH-ABO model. Also, the model known as HKH-ABO incorporates the African Buffalo Optimization (ABO) and Krill Herd Optimization (KHO) techniques. Moreover, hybridized seeks to improve illness classification precision. The CFNN model is originally created using a dataset that is a CNN's system for classifying pancreatic cancer that is based on decision trees. For categorization, regression, and some other applications, it is a collective learning technique. It works by creating classifications for various trees and creating decision trees throughout the training phase. Training and testing samples are originally separated from the 3DIRCAD dataset. Here, the technique described in Equation (3) uses test samples as follows:

$$D_{\rm s} = \{ (P_{\rm m}, Q_{\rm m}) \}, m = 1, 2, \dots N$$
 (3)

where, the pancreatic CT form numbers of patients is mentioned as $P_{\rm m} = (P^1_{m}, \dots, P^M_{m})$ with M features and the pancreatic cancer is mentioned as $Q_{\rm m}$ that includes the details about tumor like pancreatic cancerous and non-pancreatic cancerous.

Moreover, CFCNN uses mathematics to organize the data points into functional sets. Cluster the data could be tough since not every one of the elements can be examined for a huge dataset with more characteristics. So, the process can also provide the likelihood that the data point will fit into a particular category.

This network's-based process, referred as the LSTM, logically controls the cell state by excluding or integrating data using gate-like mechanisms. When the infection worsens, the degree of cancer will eventually shift. The earlier cancer data affects the current cancer size. In light of this, it would be better to combine and develop the history at earlier time steps in order to estimate the size of the malignancy. In order to avoid problems with long-term dependability, the LSTM arrangement also provides

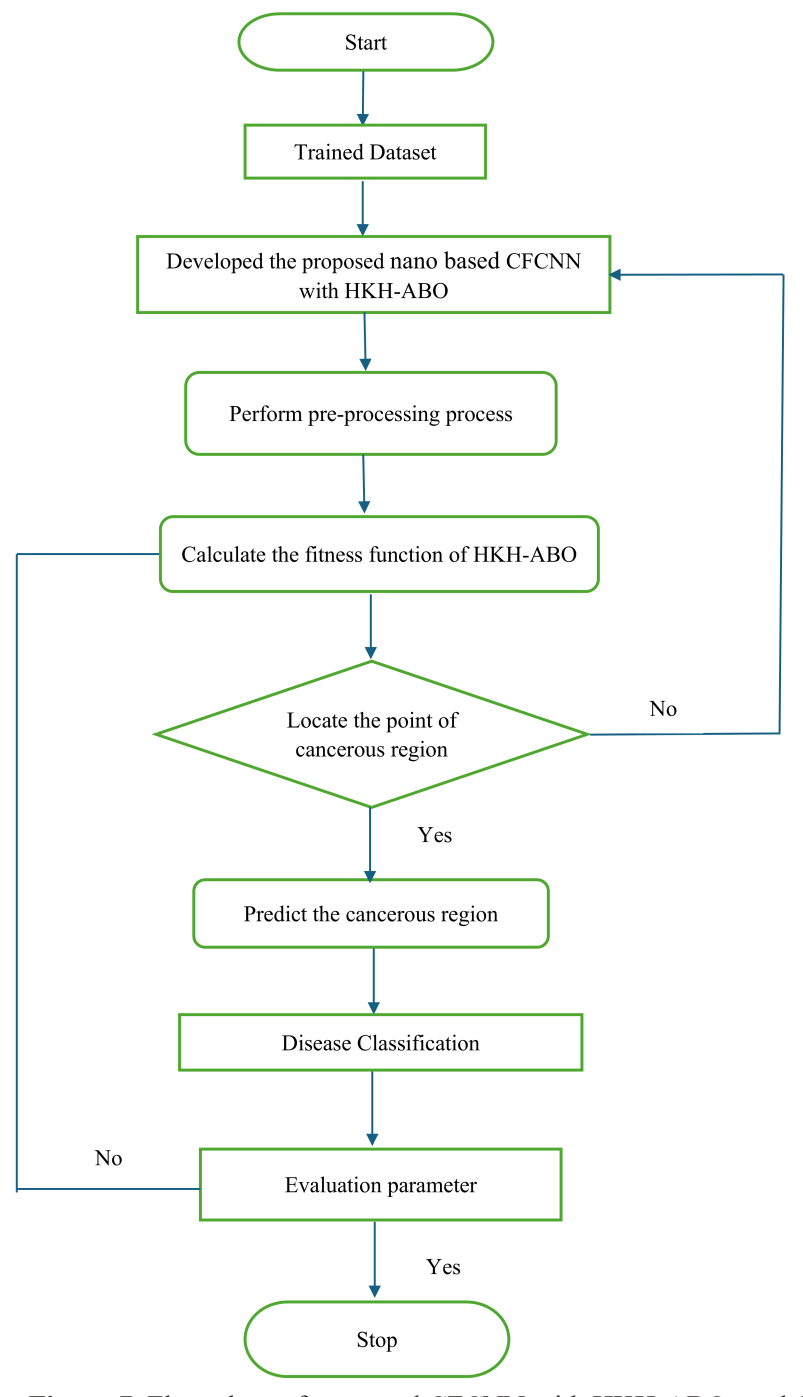


Figure 7. Flow chart of proposed CFCNN with HKH-ABO model.

a gating tool that consists of an input, concealed, and output gate. Consequently, **Figure 7**'s explanation of the developed method's entire procedure.

Let i_t to have a sigmoidal input vector as the input pattern, h_{t-1} is the result of the x is the information that was used as the output for the present step in time in equation, and t is the previous iteration step (4).

$$a1 = b + yh_{i-1} + xi_{t} (4)$$

In this, the CFCNN with HKH-ABO algorithm that analyses the diseases is given the filtering input images. The sickness characteristics are anticipated using the

trained data in Equation (2), and the second element is the output, where the imaging feature is denoted by the letter y in Equation (5),

$$h_{t} = Q_{m}(P_{m}) \tag{5}$$

Also, the illness component will be given this data, and at this layer, the HKH-ABO model creation process will begin before being transferred to the destination node. Originally, the krill herd's efficiency (K^*_{pm}) used to improve the illness categorization reported utilizing Equation (6).

$$K_{pm}^{*} = \frac{K_{f}^{*} - K_{g}^{*}}{K_{w}^{*} - K_{h}^{*}}$$
 (6)

where, K_w^* , K_b^* show each CT data's normal and abnormal features, K_f^* is the predicted normal features, and K_g^* is the predicted disease features. Let C_b be the pth patient's categorization parameter. The coefficient is well-defined in that it is more effective than other people and that it is a target I that drives the resolving to the optimization algorithm. In Equation (7), the value of C_b is defined,

$$C_b = 2\left(ran + \frac{l}{l_{max}}\right) \tag{7}$$

where l is the actual repeat amount, I_{max} is the maximum number of repetitions, and ran is a random variable between 0 and 1 that improves the searching. For each pth patient, an individualized illness prognosis is provided in Equation (8),

$$W_{f+1} = \frac{wf + m_{f+1}}{2^*} \tag{8}$$

where w_f stands for the specific case being processed, m_{f+1} stands for the features of that specific image, and training disease characteristics. As a result, the output layer receives the obtained images and produces the categorized output. As a result, Equation (9) is used to compute the output sequences of O_f (classified photos),

$$O_{\cdot} = (c^* + zh_{\cdot}) W_{c+1} \tag{9}$$

where c stands for cancerous images, h for weight of photos, t for iteration count, and z for non-cancerous images. Hence, utilizing a CT dataset, the suggested CFCNN with the HKH-ABO model has identified pancreatic cancer. Additionally, the feature extraction procedure is applied to the categorized MRI pictures in order to minimize dimensional mistakes.

3.7. Feature extraction cascaded structure for pancreatic in Kernal density estimator

The ground-truth atlas map is used to construct the cumulative distribution characteristics of the pancreatic and cancer, which display the ROI in the nearby structures. The cumulative probabilities of the pancreas for the illumination area Kernel density estimator (KDE) can be found by

$$P_{RF}^{p}(x,y,z) = \frac{1}{N_{p}W_{p}} \sum_{m=1}^{N_{p}} K \left(\frac{\left| I(x,y,z) - I^{p}(x_{m},y_{m},z_{m}) \right|}{W_{p}} \right)$$
(10)

$$K\left(\frac{V_{p}(x,y,z)-\psi op(V_{q}(x_{m},y_{m},z_{m}))}{W_{p}}\right)$$
(11)

where WP is the smoothed value, K is the Gaussian kernel function, and NP is the total number of pancreatic points in the atlas. The coordinates are denoted by x, y, and z. I(x, y, z) the strength of the volume in 3D space. A court hearing experiment was carried out on a group of 10 participants picked at random in order to achieve the best reliability, and the result was WP = 4.09. The sigma operator covers all the NP vertices of the pancreas in the atlas. The cancer density probability T is obtained by changing P(x, y, z), NP, and WP to T(x, y, z); the number of cancer locations in the atlas NT; and the cancer smoothing coefficient WT (x, y, z).

$$P_{RF}^{T}(x,y,z) = \frac{1}{N_{T}W_{T}} \sum_{m=1}^{NT} K \left(\frac{\left| I(x,y,z) - I^{T}(x_{m},y_{m},z_{m}) \right|}{W_{T}} \right)$$
(12)

$$K\left(\frac{V_{p}(x,y,z) - \psi \, oT\left(V_{q}(x_{m},y_{m},z_{m})\right)}{W_{T}}\right) \tag{13}$$

In additional to OLA map, authentic component sensitivities for the pancreatic $^{\mathrm{IP}}(x,y,z)$ and cancer $^{\mathrm{IT}}(x,y,z)$ are employed $\Psi_{\mathrm{oP}}(V_{\mathrm{q}})$ and $\Psi_{\mathrm{oT}}(V_{\mathrm{q}})$ for the detection of cancer probability map $P_{\mathrm{RF}}^{\mathrm{T}}(x,y,z)$ according to Equation (6). When utilized as a hybridization in the probabilistic map generation, the pancreatic tissue has a higher cancer voxels determination rate since it has a more unique shape and recognized architecture than a cancer. Pancreas probability map $P_{\mathrm{RF}}^{\mathrm{P}}(x,y,z)$ is made possible by a hybrid among these intensities $^{\mathrm{IP}}(x,y,z)$ and $\Psi_{\mathrm{oP}}(V_{\mathrm{q}})$ according to Equation (5).

The following formula could be used to determine whether a patch contains pancreatic voxels:

Pancreas probability =
$$\frac{P_{RF}^{P}(x, y, z)}{P_{RF}^{P}(x, y, z) + P_{RF}^{T}(x, y, z)}$$
 (14)

and the likelihood that a patch will contain cancer voxels is:

Tumor probability =
$$\frac{P_{RF}^{T}(x, y, z)}{P_{RF}^{T}(x, y, z) + P_{RF}^{P}(x, y, z)}$$
(15)

Using the ground-truth vector map, probabilistic intensity-location characteristics of the pancreas and tumor are generated, exposing the ROI inside the surrounding structures. From the location of the illumination of the pancreas, the validation number from the KDE could be determined as

Algorithm 1: Proposed nano-based pancreatic cancer classification using CFCNN with HKH-ABO

```
Input: CT pancreatic images
Output: classification using pancreatic images
Start
Int D(p,q)
dataset training
Training P<sub>m</sub>
for all P<sub>m</sub>
classification
input layer
// HKH-ABO is initiated in the hidden layer
Calculate the fitness function
Calculate P_m = W_{f+1}
Classifying the cancer types
If (C_b \le 0) then cancerous
else
If (C_{b} \le 1) then non-cancerous
end if
Extract cascaded kernal density estimator features for classification
end for
Enhanced classification accuracy
Output best solution
stop
```

To sum up, the suggested CFNNN with HKH-ABO technique successfully distinguishes between pancreatic cancerous and non-pancreatic cancerous types. Also, it improved categorization accuracy versus earlier models. The assessment ratio is 25 samples, whereas the training ratio is 600 CT images. If during the operation there are concerns with dataset unbalance, they have been corrected by moving the HKH-ABO parameter between the two levels.

3.8. Performance evaluation criteria

The suggested network's performance is evaluated using four widely used classification metrics: F1-score, accuracy, recall, and precision. These evaluation metrics can be computed using Equations (10–13) as follows:

$$Accuracy = \frac{TP + TN}{TP + FP + TN + FN}$$
 (16)

$$Precision = \frac{TP}{P + FP}$$
 (17)

F-score (%) =
$$2 \times \frac{recall \times presicion}{recall + presicion}$$
 (18)

$$Recall = \frac{TP}{TP + FN} \tag{19}$$

4. Results

The values obtained are established, and Python is used to create the proposed nano-based CFCNN using the HKH-ABO approach. The study that is being discussed aims to classify the pancreatic cancer prototype using an enhanced deep learning method. The suggested technique for recognizing pancreatic cancer includes several helpful elements, including image pre-processing, afflicted portion splitting, characteristic abstractions, and classifications.

4.1. Datasets

The dataset of CT pancreatic images is assembled, and the acquired pictures are highly processed using a unique Wien med filter to remove noise from the CT image. In order to increase classification performance with a minimal false high detection rate using the CFCNN with HKH-ABO method, cancer types are classified as either malignant or non-cancerous. Substantiated measures include accurate, recalls, precise, sensitivities, specific, and failure rate. In terms of what happened, the experimental findings were superior to the traditional model. The main factor behind this enhancement is the proposal's dual hybridized design, which combines deep learning and optimizations. So, that aids in producing the best result conceivable. During hybridization, the other computer will fix any defects in the design.

4.2. Performance analysis

The Dice index a metric of how closely the extracted shape resembles the atlas is used to assess the outcomes of CFCN extraction. **Figure 8** displays the outcomes of probability map generators for the extraction of the pancreatic and tumor shapes from a single sample slice of a CT image. The representative outcomes of the graph cut method for segmenting the pancreas. The multiplex CFCNN-HKH-ABO model, which includes a CT scan in each of the three planes (coronal, sagittal, and horizontal), does not directly employ the original clinical data images.

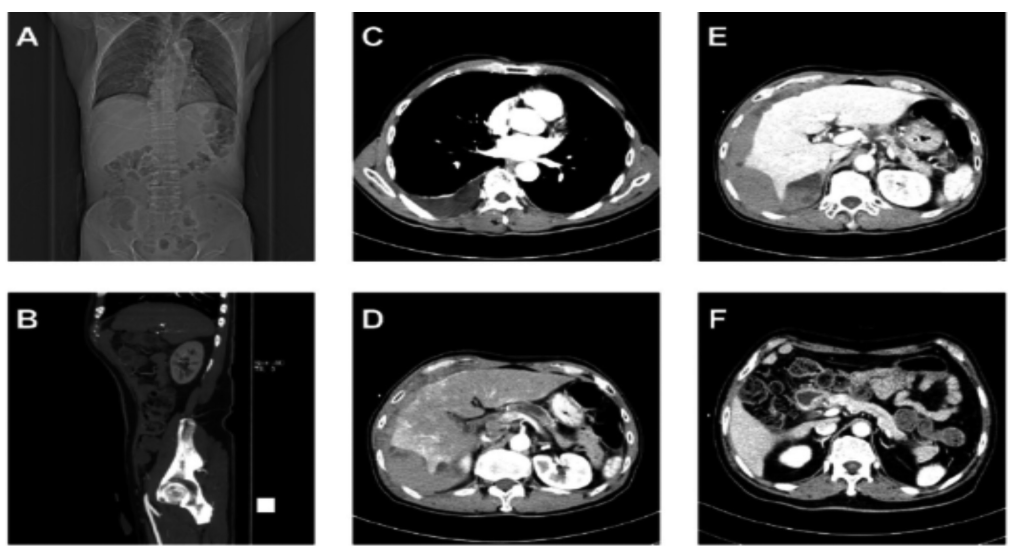


Figure 8. CT scans in the coronal plane (A), dagget (B), and without the pancreatic (C), aortic (D), microvascular (E), and disrupted phase CT images.

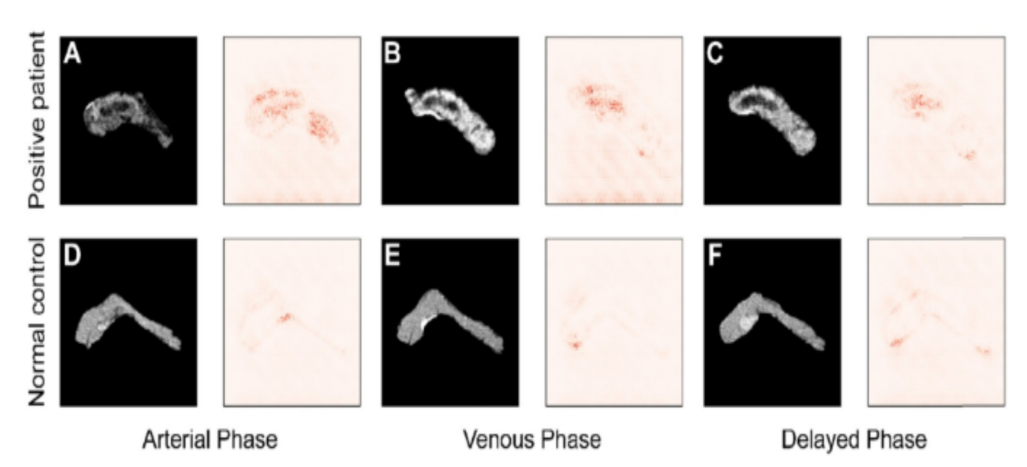


Figure 9. Comparison of salience maps for (A, B, and C) are cancer patients and (D, E, and F) are non-cancerous patients.

By calculating the derivatives of the right class scores with reference to the picture pixels and emphasizing the regions that the neural network considers most important, a saliency map increases the accuracy of the designer's diagnoses. It can help radiologists grasp the desktop decision by serving as a graphical analysis tool, which raises the model's confidence. **Figure 9** shows a comparison of salience maps.

Figure 10 shows the biomarker results in pancreatic tumor classification. Biomarker-based pancreatic cancer screening could significantly improve survival rates in appropriately targeted high-risk patients. Prior to analysis, samples from each group were randomly assigned to training and blinded validation sets. To discover discriminatory biomarker panels in the training set, we employed a CFCNN with the HKH-ABO algorithm. The identified panels were tested in a validation set as well as in colon cancer patients.

In this paper, introduced the effectiveness of the proposed nano-based CFCNN with HKH-ABO technique can classify the important indicators in this section. The

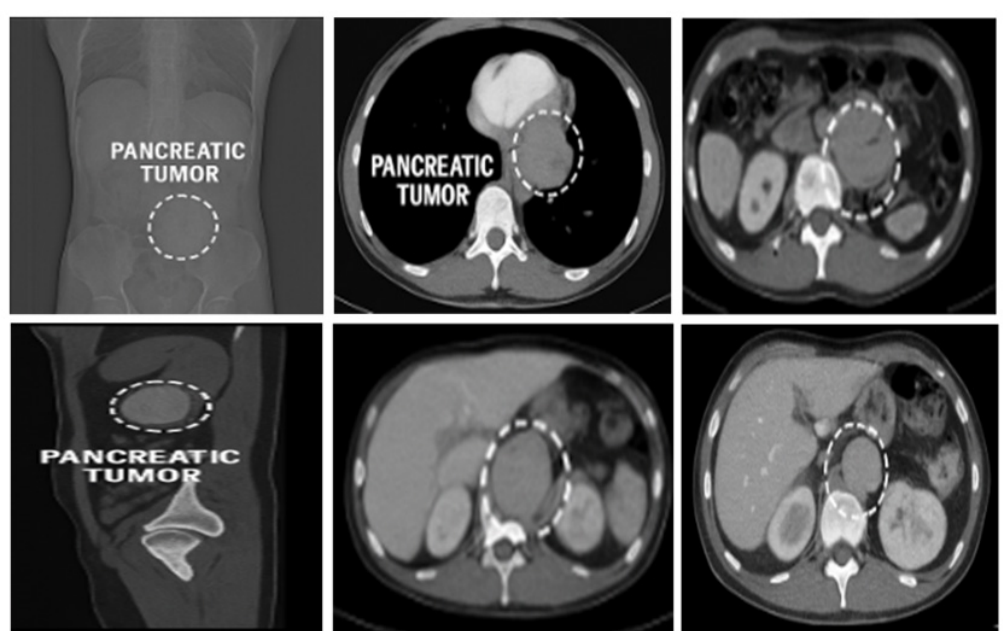


Figure 10. Biomarker results in pancreatic tumor classification.

suggested model was evaluated using some commonly employed performance metrics: Confusion matrix, Roc, and AUC curve as some evaluation parameter, such as accuracy, precision, recall, error rate, specificity, and sensitivity. Finally compared some existing method with proposed method to perform better accuracy.

5. Discussion

5.1. A potential DNA methylation biomarker for early identification of pancreatic cancer

The aberrant methylation status of BNC1 and ADAMTS1 was determined by quantitative MSP analyses, as shown in Figure 11A and linked with gene expression patterns using qPCR (Figure 11B). In these cell lines, both genes demonstrated a lack of endogenous gene expression followed by considerable re-expression after DAC treatment. Treatment with TSA, a histone deacetylase inhibitor, resulted in limited re-expression except for BNC1 in PL45, which may be regulated by promoter DNA methylation and histone modifications, as shown in Figure 2B. Bisulfite sequencing verified CpG island methylation in the BNC1 and ADAMTS1 promoters in pancreatic cancer cell lines, primary pancreatic cancer tissues, normal pancreatic tissue, and the DNMT1(/) DNMT3B (/) double knockout (DKO) as a negative control. These findings demonstrated that BNC1 and ADAMTS1 were densely methylated in the pancreatic cancer cell line and primary pancreatic cancer, but normal pancreas tissues and DKO had minimal or no methylation. These findings are consistent with both the conventional and quantitative MSP analyses, as shown in Figure 11C and D.

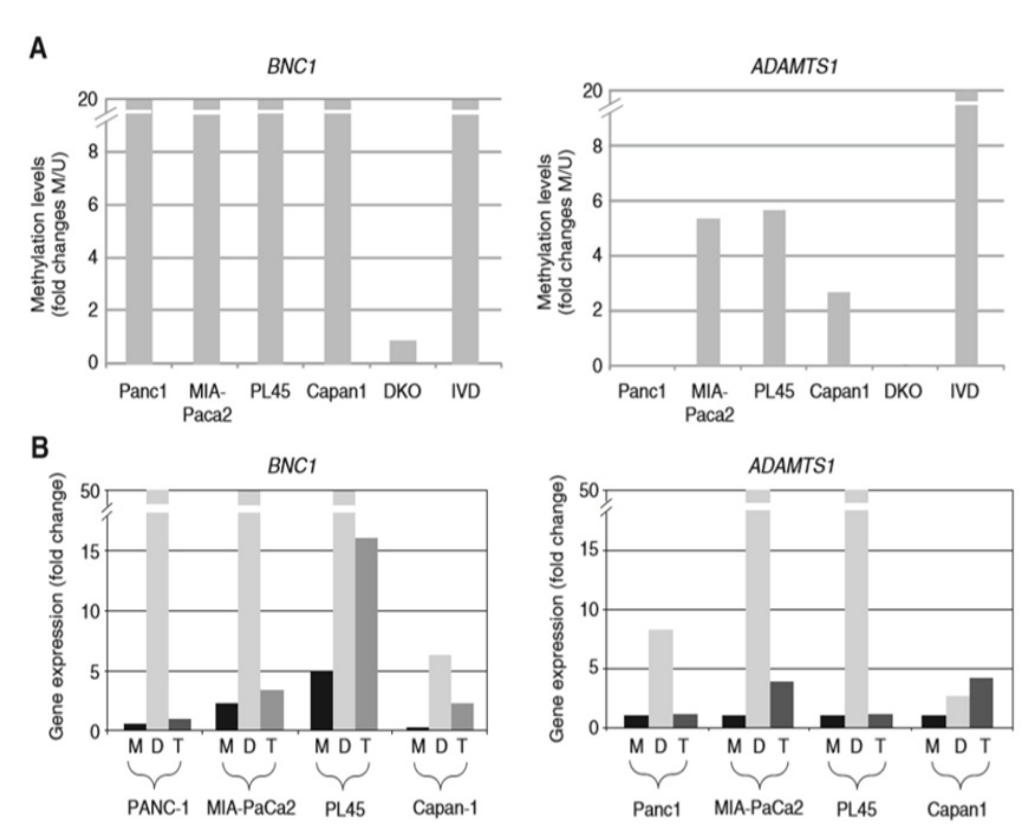


Figure 11. Silencing of BNC1 and ADAMTS1 genes biomarker in pancreatic cancer cell lines.

5.2. Confusion matrix

The confusion matrix is used to demonstrate how well the presented technique performed across both datasets. The confusion matrix provides additional evidence of the proposed method's classification results in regards to the actual and projected class. **Figure 12** shows the discriminant function that was discovered throughout the simulation phase.

Patterson's link results demonstrate how feature attributes influence objective attributes. In **Figure 13** despite the main attributes associated with patient attributes, no single statistic has a significant impact on stroke, according to covariance matrices. Age, gender, overall survival, disease free survival, pancreatic stage 1, stage 2, stage 3, stage 4, pmax diameter (cm), and differentiation all have an impact on pancreatic cancer.

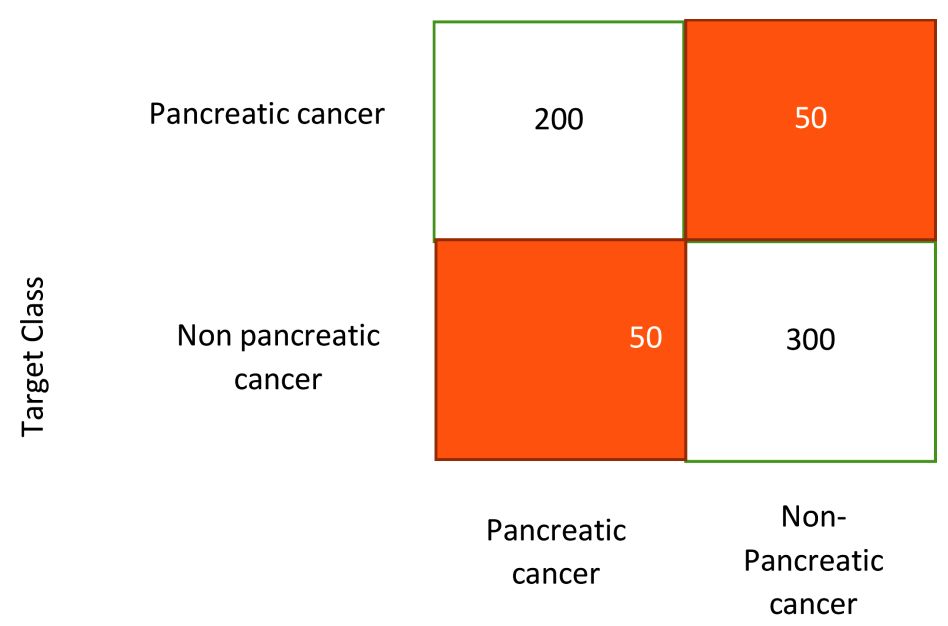


Figure 12. Confusion matrix.

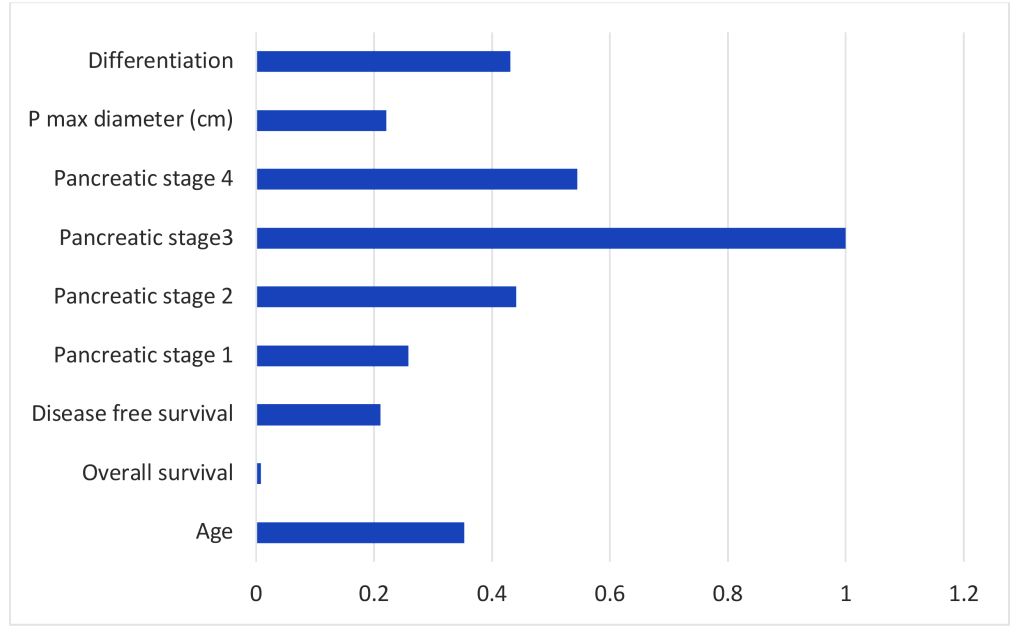


Figure 13. Clinical dataset for pancreatic cancer.

5.3. Samples for training, validating, and evaluating

The training/validation (n = 50, evaluated by an imaging professional [VA]) and testing (n = 10) subsets of the CT 3DIRCAD dataset were created. The algorithms were trained and validated using 600 validation samples. The validation dataset was then subjected to the trained and verified algorithms.

In its final output, the proposed method employs 600 samples. **Figure 14** depicts the accuracy as a function of epoch count in both validation and training, while **Figure 15** depicts the corresponding loss.

The related values are shown in **Table 1**. After feature extraction, valid photos were randomized split into three groups with a ratio of 6:2:2 for learning, verifying, and evaluating each thread, respectively. Training was halted while neither efficiency nor loss continued to improve.

It evaluated the approaches used by ResNet-32, OLA, OLA + PL-MRCNN, and Cascaded Fully Connected Neural Network (CFCNN). OLA, OLA + PL-MRCNN,

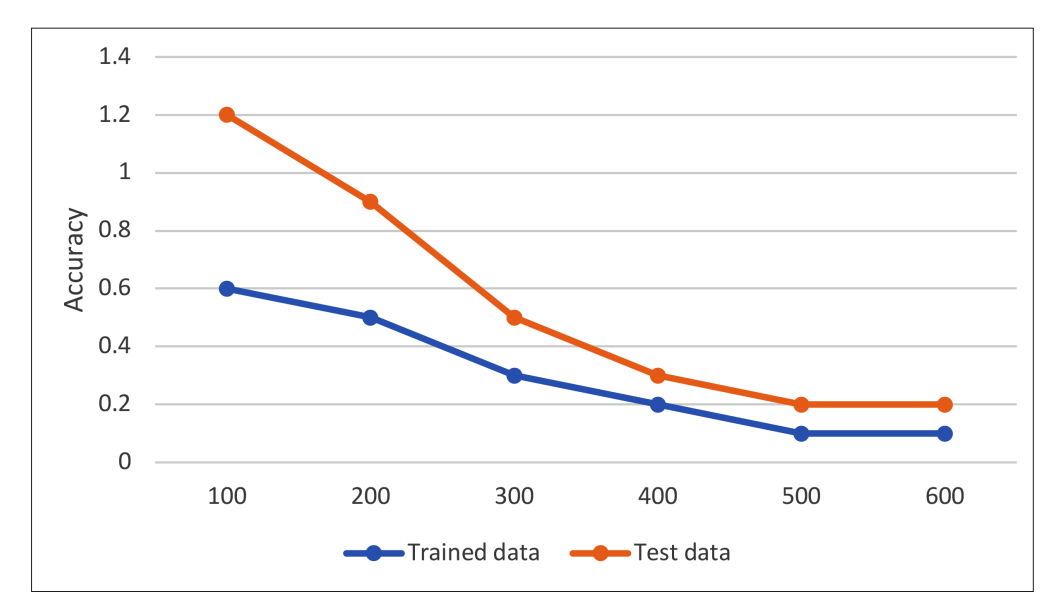


Figure 14. Accuracy versus samples.

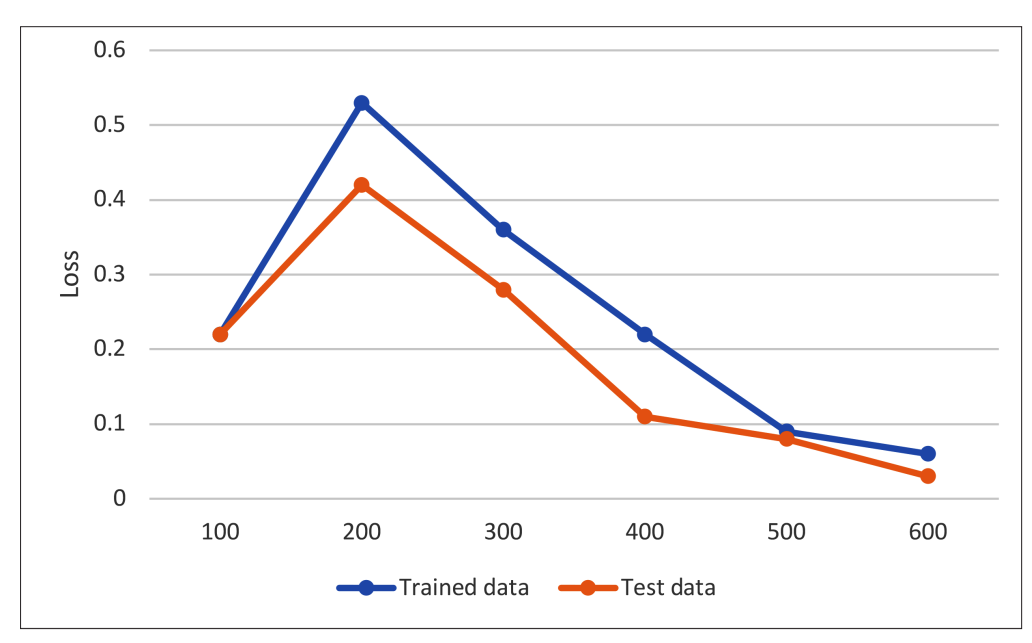


Figure 15. Loss versus samples.

707 1 1 4	D C	C .1 1	1 1
Tabla	Partormanca	at the trained	and test dataset.
Table 1.	. i ci ioi illancc	or the trained	and itsi dalasti.

Models	Samples	Training accuracy	Validation accuracy (%)	Testing accuracy (%)	Training loss
OLA	200	87.8	88.12	91.12	5.1
OLA + PL- OLA + PL- MRCNN	20	89.45	87.12	94.87	2.01
ResNet-32	300	90.02	88.17	85.36	1.25
Proposed nano-based CFCNN with HKH-ABO	600	97.14	84.16	96.99	0.03

ResNet-32, and completely cascaded all contrast the graph-cut approach and wavelet filtering. The mixture of OLA and PL-MRCNN is referred to as OLA + PL-MRCNN. After using OLA, OLA + PL MRCNN, ResNet-32, and the fully cascaded technique, the pancreas shape extraction DSCs increased from 97%, 88.17%, and 96.99% MLoU to 90.02%, 84.16%, and 97.14%, correspondingly.

5.4. ROC and AUC curves

Figure 16 depicts the ROC curves used to contrast the suggested CFCNN with the HKH-ABO hybrid approach. There are several curves that may be produced by displaying the graph on the y-axis and the false-positive rate on the x-axis. By changing the cut-off value, these curves investigate the model's score in the interim. When the area under the curve (or ROC) is big, it clearly illustrates that performance improves. It is important to remember that the AUC may exceed 0.98 for all categories.

The proposed nano-based CFCNN with HKH-ABO outperformed deep learning hybrid optimization techniques. The accuracy rate, precise, specificity, sensitivity, recollect, and failure rate of the proposed nano-based CFCNN with HKH-ABO are evaluated to those of four current models in **Table 2**. Using established methods like Firefly modified chicken-based Chicken Swarm Optimization with Convolutional RNN (FC-CSO-CRNN), Optimized Artificial Neural Network (OANN), and MVO-GBDT, the effectiveness of the proposed strategy is confirmed.

In **Figure 17**, the error rate of the developed CFCNN with the HKH-ABO low error rate 0.12% approach is validated against existing approaches. The prevalent methods, such as FC-CSO-CRNN, OANN, and MVO-GBDT approaches, have high error rates of 1.6%, 1.1%, and 0.91%, respectively.

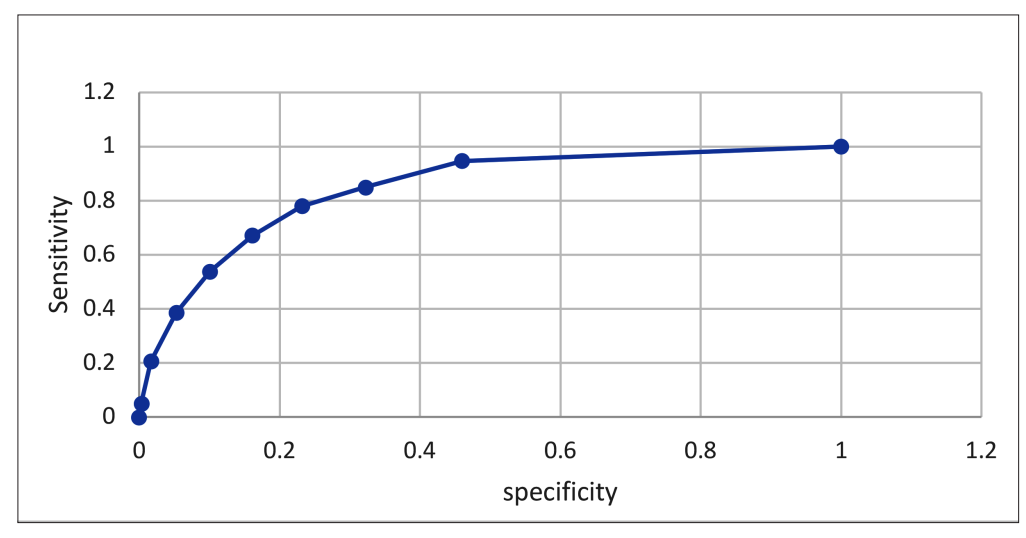


Figure 16. ROC under AUC curve.

Table 2. Classification of proposed nano-based CFCNN with HKH-ABO technique.

Methods	Average accurate	Precision	Specificity	Sensitivity	Recollect	Failure rate
RNN (FC-CSO- CRNN)	95.52	92.01	91.22	95.85	75	1.6
Optimized Artificial Neural Network (OANN)	96.22	93.12	94.12	93.21	82	1.1
MVO-GBDT	97.14	95.12	95.35	94.17	83	0.91
Proposed nano-based CFCNN with HKH-ABO	98.87	96.27	98.22	95.78	96.11	0.12

In **Figure 18**, the failure rate of the proposed nano-based CFCNN with the HKH-ABO low error rate 0.12% approach is validated against existing approaches. The prevalent methods, such as FC-CSO-CRNN, OANN, and MVO-GBDT approaches, have high failure rates of 1.6%, 1.1%, and 0.91%, respectively.

Figure 19 shows a comparison of the precision, specificity, and sensitivity. Table 3 compares the best outcomes obtained utilizing the advised hybrid approach

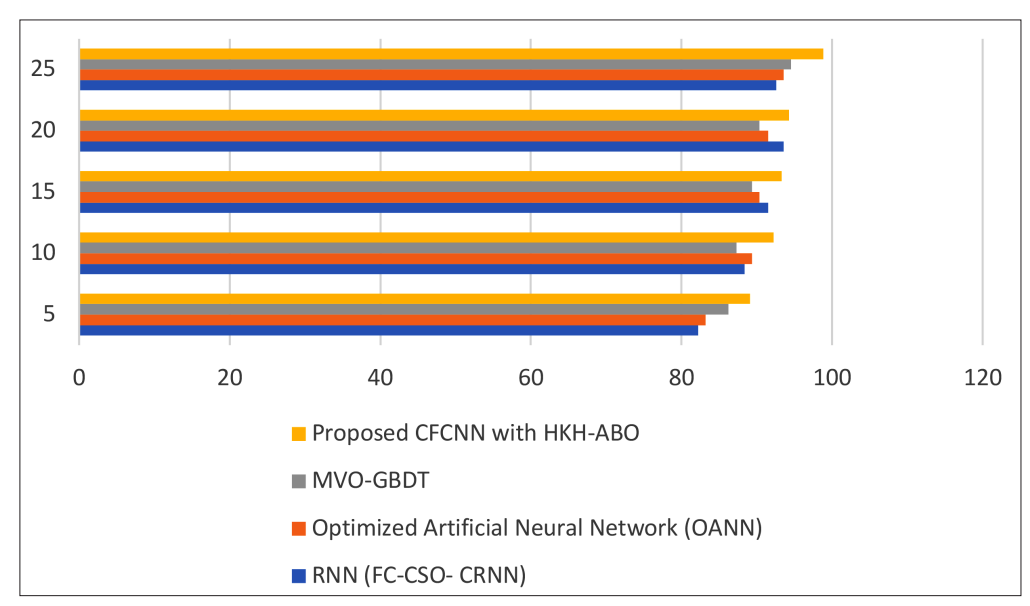


Figure 17. Accuracy.

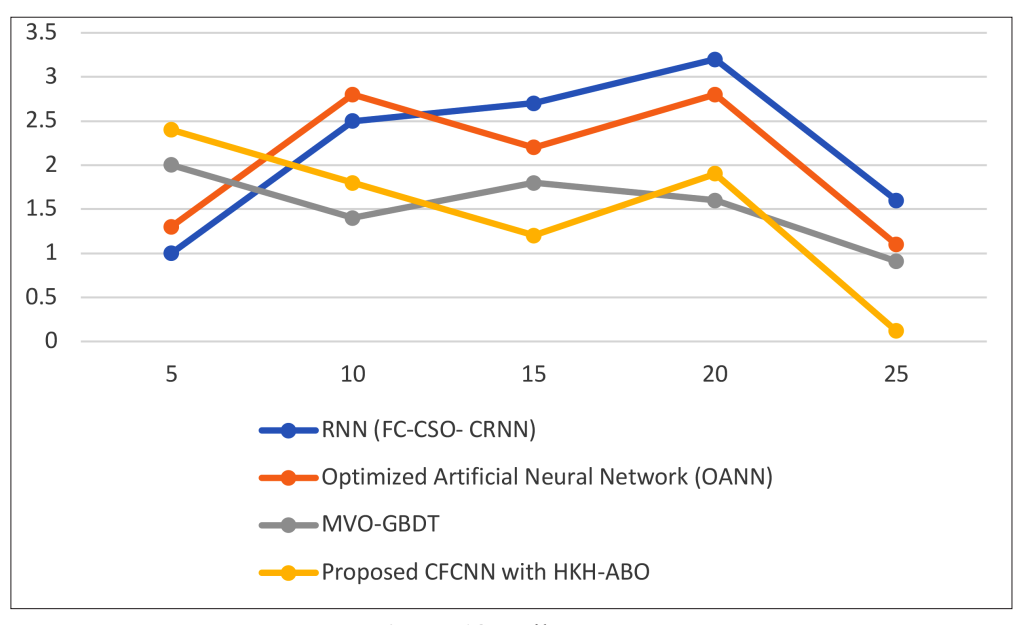


Figure 18. Failure rate.

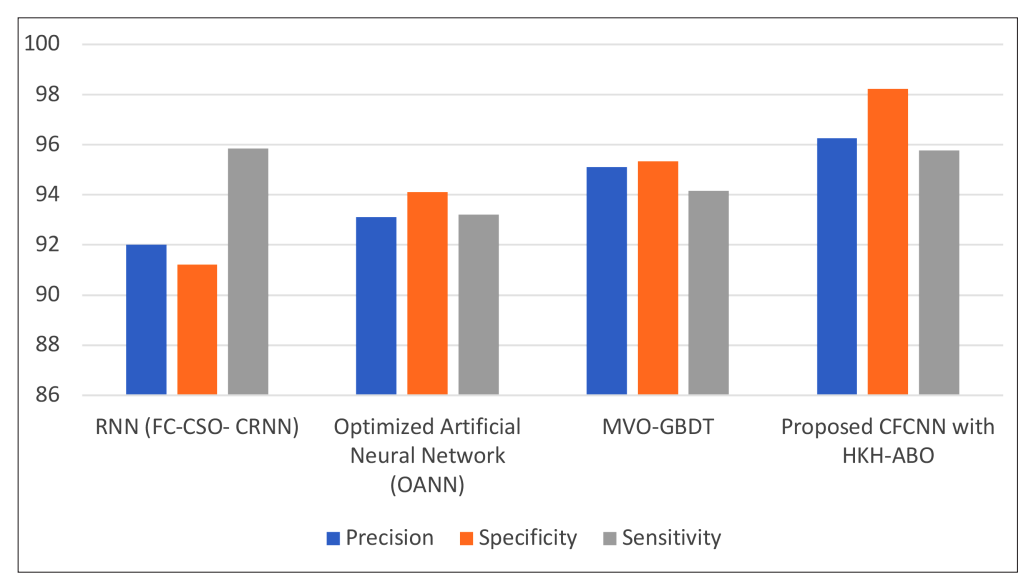


Figure 19. Comparative of sensitivity, specificity, and precision.

to those of other researchers that have previously publicized their work in order to emphasize the distinctions between hybrid and other improvements. This served as the basis for the proposed HKH-ABO framework. According to the results, the proposed system surpasses the current ones with a represent the greatest of 98.22%. Lastly, the suggested approach determined the presented in tabular form based on the quantity of trained photos evaluated using existing techniques. The existing methods achieved able to make decisions based of nearly 95.85% for FC-CSO-CRNN, 93.21% for OANN, and 94.17% for MVO-GBDT. In terms of sensitivity, the findings indicate that the suggested scheme outperforms the existing ones (95.78%).

5.5. Comparison with existing techniques

The suggested CFCNN with HKH-ABO methodology accomplished a 0.12% error rate in characterizing pancreatic cancer. The consolidated HKH and ABO models perform poorly in categorizing pancreatic cancer. These methods' hybrid forms are highly efficient. Moreover, in the interest of maximizing effectiveness, these optimization algorithms are carried out in an identical environment. To highlight the differences between hybrid and other enhancements, **Table 3** compares the best results produced using the recommended hybrid technique to those of other researchers who have already published their work. The suggested HKH-ABO model was inspired by this.

As a result, as shown in **Table 3**, the designed CFCNN with HKH-ABO model classified pancreatic cancer at an early stage with good accuracy, sensitivity, preci-

Methods Accurate Precision Recollect Failure Author **Specificity** Sensitivity **Rate (%)** (%)(%)(%) (%) (%)92.1 Zhenget al. (2020) **DLA-EABA** 96.2 93.92 92.8 98.3 1.8 Zhang et al. (2021) **CNN** 78 86 77 80 86 10 Piantadosi et al. (2022) 97.11 94.16 92.34 93.49 92.80 0.74 Deep CNN CFCNN with HKH-ABO 96.27 98.22 95.78 96.11 0.12 Proposed work 98.87

Table 3. Comparison with existing techniques.

sion, recall, specificity, and a lower error rate. When compared to all existing models, the proposed model outperformed them in all specifications.

6. Conclusion

BNC1 and ADAMTS1 is a potential biomarker to detect early-stage pancreatic cancers. Assaying the promoter methylation status of these genes in circulating DNA from serum is a promising strategy for early detection of pancreatic cancer and has the potential to improve mortality from this disease. This research showed that using CFNN in combination with HKH-ACO on hepatic portal CT images can accurately differentiate pancreatic cancer. The CFNN model may be used as a computer-aided diagnostics tool to help doctors and medical students make a pancreatic cancer diagnosis. The obtained collection of CT images is initially used to develop the system. The faults related to conditioning and strength training were then eliminated using the pre-process tool. In order to complete the characteristic extraction and classification features, the pre-processed data were then put into the classification algorithm. According to the outcomes of the suggested model, pancreatic cancer can be divided into subgroups that are both pancreatic cancerous and non-pancreatic cancerous. Also, the suggested scheme's performance was contrasted with that of other current schemes in terms of a number of criteria, including accuracy, recall, sensitivity, precision, and error rate. As a result, the model's usefulness was demonstrated by the possible new framework 98.87% greater accuracy and 0.12% reduced failure rate. The nano-based cancer images are an effective diagnostic approach and classified to detect cancer cells. It measures the size, color, and shape of the cancer cell. Different kinds of tumors can be identified, along with the position of the tumor and to calculate tumor growth.

Author contributions: Conceptualization, SRP and STS; methodology, SRP; software, SRP; validation, SRP and STS; formal analysis, STS; investigation, STS; resources, SRP; data curation, SRP; writing—original draft preparation, SRP; writing—review and editing, SRP; visualization, STS; supervision, STS; project administration, STS; funding acquisition, STS. All authors have read and agreed to the published version of the manuscript.

Funding: This research received no external funding.

Acknowledgment: The author would like to express their heartfelt gratitude to the supervisor for his guidance and unwavering support during this research.

Ethical approval: Not applicable.

Informed consent statement: Not applicable.

Conflict of interest: The authors declare no conflict of interest.

References

Brozos-Vázquez, Elena Marta Toledano-Fonseca, Nicolás Costa-Fraga, et al. Pancreatic cancer biomarkers: A
pathway to advance in personalized treatment selection. Cancer Treatment Reviews. 2024; 125: 102719. doi:
10.1016/j.ctrv.2024.102719

- 2. Li H, Zhong H, Boimel PJ, et al. Deep convolutional neural networks for imaging-based survival analysis of rectal cancer patients. International Journal of Radiation Oncology. 2017; 99(2): S183.
- 3. Yasaka K, Abe O. Deep learning and artificial intelligence in radiology: Current applications and future directions. PLoS Medicine. 2018; 15: e1002707. doi: 10.1371/journal.pmed.1002707
- 4. Esteva A, Kuprel B, Novoa RA, et al. Dermatologist-level classification of skin cancer with deep neural networks. Nature. 2017; 542: 115–18. doi: 10.1038/nature21056
- Chithra PL, Bhavani P. Nanotechnology Perspective of Lung Cancer Imaging Diagnosis using Deep Learning Techniques. In: 2022 6th International Conference on Trends in Electronics and Informatics (ICOEI), 1393–1398. IEEE, 2022. R. Madadjim, Using an integrative machine learning approach to study microRNA regulation networks in pancreatic cancer progression; 2021.
- 6. Al-Fatlawi A, Malekian N, García S, et al. Deep learning improves pancreatic cancer diagnosis using rnabased variants. Cancers. 2021; 13(11): 2654. doi: 10.3390/cancers13112654
- 7. Tonozuka R, Itoi T, Nagata N, et al. Deep learning analysis for the detection of pancreatic cancer on endosonographic images: A pilot study. Journal of Hepato Biliary Pancreatic Sciences. 2021; 28(1): 95–104. doi: 10.1002/jhbp.825
- 8. Poce I, Arsenjeva J, Kielaite-Gulla A, et al. Pancreas segmentation in CT images: State of the art in clinical practice. Baltic Journal of Modern Computing. 2021; 9(1): 25–34. doi: 10.22364/bjmc.2021.9.1.02
- 9. Lara JA, Lizcano D, Valente JP et al. A general framework for time series data mining based on event analysis: Application to the medical domains of electroencephalography and stabilometry. Baltic Journal of Biomedical Informatics. 2014; 51: 219–241. doi: 10.1016/j.jbi.2014.06.003
- 10. Muhammad W, Hart GR, Nartowt B, et al. Pancreatic cancer prediction through an artificial neural network. Frontiers in Artificial Intelligence. 2019; 3: 2. doi: 10.3389/frai.2019.00002
- 11. Appelbaum L, Cambronero JP, Stevens JP, et al. Development and validation of a pancreatic cancer risk model for the general population using electronic health records: An observational study. European Journal of Cancer. 2021; 143: 19–30. doi: 10.1016/j.ejca.2020.10.019
- 12. Zhang M, Shi X, Wu C, et al. Identification of reliable biomarkers for radiation pneumonia using a proteomics approach. Journal of Biological Regulators and Homeostatic Agents. 2023; 37(10): 5175–5186. doi: 10.1007/s00432-023-04827-7
- 13. Zhang CW, Jia DY, Wu NK, et al. Quantitative detection of cervical cancer based on time series information from smear images, Applied Soft Computing. 2021; 112(03): 107791. doi: 10.1016/j.asoc.2021.107791
- 14. Wang S, Celebi ME, Zhang Y, et al. Advances in data preprocessing for biomedical data fusion: An overview of the methods, challenges, and prospects, inform. Fusion. 2021; 76: 376–421. doi: 10.1016/j.inffus.2021.07.001
- 15. Azad TD, Ehresman J, Ahmed AK, et al. Fostering reproducibility and generalizability in machine learning for clinical prediction modeling in spine surgery. The Spine Journal. 2020; 21(10): 1610–1616. doi: 10.1016/j.spinee.2020.10.006
- 16. López-Zambrano J, Lara JA, Romero C. Improving the portability of predicting students' performance models by using ontologies. Journal of Computing in Higher Education. 2022; 34(1): 1–19. doi: 10.1007/s12528-021-09273-3
- 17. Gutiérrez R, Rampérez V, Paggi H, et al. On the use of information fusion techniques to improve information quality: Taxonomy, opportunities and challenges, Inform Fusion. 2022; 78: 102–137. doi: 10.1016/j.inffus.2021.09.017
- 18. Farag A, Lu L, Roth HR, et al. A bottom-up approach for pancreas segmentation using cascaded superpixels, and (Deep) image patch labeling. IEEE Transactions on Image Processing. 2017; 26(1): 386–399. doi: 10.1109/TIP.2016.2624198
- Jain S, Gupta S, Gulati A. An adaptive hybrid technique for pancreas segmentation using CT image sequences.
 In: Proceedings of the 2015 International Conference on Signal Processing, Computing and Control (ISPCC); 24–26
 September 2015; Waknaghat, India. pp. 272–276. doi: 10.1109/ISPCC.2015.7375039
- 20. Gibson E, Giganti F, Hu Y, et al. Automatic multi-organ segmentation on abdominal CT with dense V-Networks. IEEE Transactions on Medical Imaging. 2018; 37(8): 1822–1834. doi: 10.1109/TMI.2018.2806309
- 21. Erdt M, Kirschner M, Drechsler K, et al. Automatic pancreas segmentation in contrast enhanced CT data using learned spatial anatomy and texture descriptors. In: Proceedings of the 2011 IEEE International Symposium on Biomedical Imaging: From Nano to Macro; 30 March 2011–2 April 2011; Chicago, IL, USA. pp. 2076–2082. doi: 10.1109/ISBI.2011.5872821
- 22. Shimizu A, Kimoto T, Kobatake H, et al. Automated pancreas segmentation from three-dimensional contrast enhanced computed tomography. International Journal of Computer Assisted Radiology and Surgery. 2010; 5(1): 85–98. doi: 10.1007/s11548-009-0384-0.

- 23. Wolz R, Chu C, Misawa K, et al. Automated abdominal multi-organ segmentation with subject-specific atlas generation. IEEE Transactions on Medical Imaging. 2013; 32(9): 1723–1730. doi: 10.1109/tmi.2013.2265805
- 24. Taha AA, Hanbury A. Metrics for evaluating 3D medical image segmentation: Analysis, selection, and tool. BioMed Central Medical Imaging. 2015; 15: 29. doi: 10.1186/s12880-015-0068-x
- 25. Okada T, Linguraru M, Yoshida Y, et al. Abdominal multi-organ segmentation of CT images based on hierarchical spatial modeling of organ interrelations. In: Proceedings of the Third International Workshop on Abdominal Imaging: Computational and Clinical Applications; 18 September 2011; Toronto, Canada. pp. 173–180. doi: 10.1007/978-3-642-28557-8 22
- 26. Chu C, Oda M, Kitasaka T, et al. Multi-organ segmentation based on spatially-divided probabilistic atlas from 3D abdominal CT images. In: Proceedings of the 16th International Conference on Medical Image Computing and Computer-Assisted Intervention–MICCAI 2013; 22–26 September 2013; Nagoya, Japan. pp. 165–172. doi: 10.1007/978-3-642-40763-5 21
- 27. Park J, Artin MG, Lee KE, et al. Deep learning on time series laboratory test results from electronic health records for early detection of pancreatic cancer. Journal of Biomedical Informatics. 2022; 131: 104095. doi: 10. 1016/j.jbi.2022.104095
- 28. Placido D, Yuan B, Hjaltelin JX, et al. Pancreatic cancer risk predicted from disease trajectories using deep learning. Preprint at bioRxiv. 2022. doi: 10.1101/2021.06.27.449937.
- 29. Brachi G, Bussolino F, Ciardelli G, et al. Nanomedicine for imaging and therapy of pancreatic adenocarcinoma. Frontiers in Bioengineering and Biotechnology. 2019; 7: 307. doi: 10.3389/fbioe.2019.00307